Joule

CellPress

Article

Combining Reclaimed PET with Bio-based Monomers Enables Plastics Upcycling

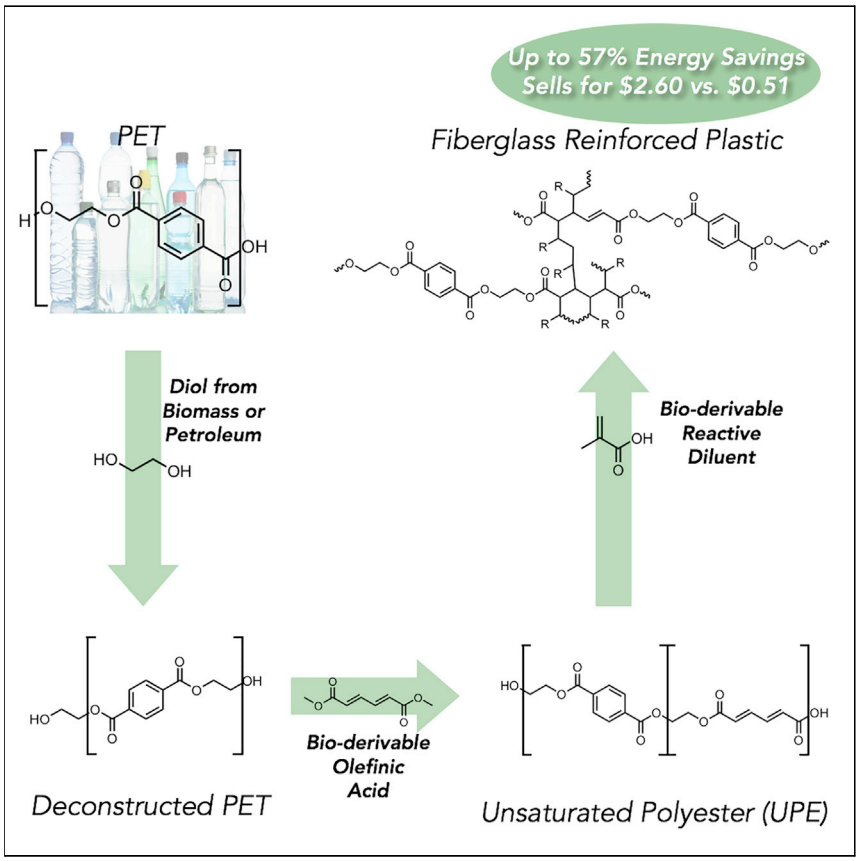

This study develops an approach to incentivize both higher extents of waste plastics reclamation and use of bio-based chemicals. In particular, reclaimed plastics (polyethylene terephthalate) and chemicals derivable from renewable resources are combined to create high-performance, long-lifetime composite materials with properties that exceed those of standard petroleum-based materials and that exhibit higher selling prices than reclaimed plastic. Analysis predicts that this approach results in reductions in energy input and greenhouse gas emissions relative to standard composites manufacturing today.

Nicholas A. Rorrer, Scott Nicholson, Alberta Carpenter, Mary J. Biddy, Nicholas J. Grundl, Gregg T. Beckham

gregg.beckham@nrel.gov

HIGHLIGHTS

Upcycling is the ability to produce higher-value products from reclaimed material

Recycled PET is combined with bio-based monomers to incentivize plastics reclamation

Upcycling with bioderived monomers results in materials with superior properties

These upcycled materials result in lower production energy and GHG emissions

Rorrer et al., Joule 3, 1006–1027
April 17, 2019
https://doi.org/10.1016/j.joule.2019.01.018

Joule

CellPress

Article

Combining Reclaimed PET with Bio-based Monomers Enables Plastics Upcycling

Nicholas A. Rorrer,[1] Scott Nicholson,[2] Alberta Carpenter,[2] Mary J. Biddy,[1] Nicholas J. Grundl,[1] and Gregg T. Beckham[1,3,*]

SUMMARY

Polyethylene terephthalate (PET) is the largest produced polyester globally with an annual production exceeding 26 million tons for use in carpet, clothing, and single-use beverage bottles, among others. Today, only PET bottles are reclaimed for recycling, albeit at a low reclamation rate, with most of the waste PET accumulating in landfills or the environment. In this study, PET is upcycled to higher-value, long-lifetime materials, namely two types of fiber-reinforced plastics (FRPs), via combination with renewably sourceable monomers. By harnessing the embodied energy in reclaimed PET (rPET) and implementing renewably sourceable monomers with distinct chemical functionality relative to petroleum building blocks, the resultant rPET-FRPs exhibit considerably improved material properties and are predicted to save 57% in the total supply chain energy and reduce greenhouse gas emissions by 40% over standard petroleum-based FRPs. Overall, this study enables a route to PET upcycling via bio-based monomers that could incentivize both improved plastics reclamation and acceleration of the bioeconomy.

INTRODUCTION

Polyethylene terephthalate (PET) is the largest produced polyester and fourth largest produced polymer in the world today.[1] PET is used across many economic sectors for many applications owing to its advantageous properties, namely low permeability, low weight, and high stain resistance.[2] The current worldwide production of PET exceeds 26 million tons per year, with 60% finding use as synthetic fibers (e.g., carpet) and 30% employed in single-use beverage bottles.[3–5] Despite robust recycling programs in many countries, the predominance of single-use PET contributes substantially to the 6.3 billion tons of total plastic waste in landfills,[1] a high terrestrial prevalence of microplastics,[6–8] and high rates of plastics accumulation in the ocean.[9,7] Despite the ability of PET bottles to be recycled, no country in the world reclaims more than 60% of their PET bottles for recycling, with most countries averaging 30%.[3,10,11] Overall, less than 15% of PET bottles find a second life, typically being utilized at low loading in virgin materials or in fibers.[3]

Most industrialized recycling technologies today rely on mechanical methods for PET recycling,[12–14] which leads to a 30% reduction in value owing to the reduction in properties of recycled PET relative to virgin PET.[15–18] Alongside the contaminants present in the recycling stream (such as other plastics, adhesives, and debris), mechanical recycling techniques result in molecular weight reduction and chemical inhomogeneity.[4] Recycled polymers also often lose optical clarity. In certain cases, recycled PET can be blended with virgin PET at loadings of less than 30%, and sufficient properties for PET bottles can still be maintained. The loss of value

Context & Scale

PET is a ubiquitous material because of its robust properties. Today, less than 30% of PET bottles and few carpets are recycled in the United States, leading to the majority of PET being landfilled. The low PET reclamation rate is due to the fact that PET bottle recycling today is mechanical, resulting in a devalued product. Here, reclaimed PET (rPET) bottles are converted to fiberglass-reinforced plastics (FRPs), which sell for more than twice that of rPET. When monomers derivable from biomass are incorporated, rPET-FRPs with superior properties are achieved. Supply chain energy calculations reveal that this strategy for plastics upcycling could save significant total manufacture energy, mainly from savings in associated energy from petroleum feedstocks, and could also reduce greenhouse gas emissions. Overall, this approach provides an economic incentive for plastics recycling and renewable feedstock use through the creation of long-lifetime, performance-advantaged materials.

Table 1. Number Average Molecular Weight after Deconstruction of PET Using a Transesterification Catalyst, Titanium Butoxide at 0.5 wt %, in Excess Ethylene Glycol or Butanediol under Reflux (T = ~220°C) for 4 h

Mass Ratio (Diol:PET)	Ethylene Glycol		Butanediol	
	Molecular Weight (g/mol)	Đ	Molecular Weight (g/mol)	Đ
0	5.7×10^4	1.12	5.7×10^4	1.12
0.125	5.3×10^4	1.15	5.6×10^4	1.16
0.25	5.0×10^4	1.15	5.3×10^4	1.15
0.5	4.7×10^4	1.37	4.9×10^4	1.39
1.0	3.2×10^4	1.41	3.1×10^4	1.42
2.0	1.5×10^4	1.53	1.6×10^4	1.57
4.0	7.2×10^3	1.79	7.6×10^3	1.81

associated with mechanical recycling thus leads to the underutilization of PET bottles as a feedstock for recycling.

While mechanical recycling has found industrial use, there is an ongoing effort to develop more effective ways to chemically recycle PET.[19,20] Chemical recycling, unlike mechanical recycling, is typically focused on converting PET to versions of its monomeric precursors such as terephthalic acid and ethylene glycol, dimethyl terephthalate and ethylene glycol, or bis-hydroxy(2-ethyl) terephthalate (BHET). Similar to mechanical recycling, contaminants from the used PET can affect the process, requiring more energy-intensive, costly separations. Unlike mechanical recycling, however, the monomers can be purified, ultimately leading to resynthesized PET that exhibits properties identical to virgin plastic. A majority of catalytic methods require expensive catalysts or extensive reactor times to deconstruct the polymer.[20] To date, ionic liquids with low catalyst loadings are able to achieve complete deconstruction of PET in a short amount of time[21] and are in the initial stages of implementation. Additionally, further developments in organocatalysis have demonstrated promise to effectively produce BHET using volatile catalysts.[22–25] Further details about the catalytic deconstruction of PET can be found in a series of reviews.[4,18–20,26,27]

While there are some benefits to the complete deconstruction of PET, the partial deconstruction of PET can also lead to its use in other applications owing to the properties that make it favorable as a homopolymer, namely high strength and near-ideal thermal properties. To date, partially depolymerized PET has found use in epoxy resins,[29,30] polyurethanes,[28] and unsaturated polyesters (UPEs).[31–35] These products are ideal for utilizing recycled plastics as feedstocks because they can command a higher selling price than virgin PET and their market sizes are continuously growing.[36] However, in all previous work, recycled PET has been highly deconstructed (which requires a greater energy input) and combined with toxic monomers such as epichlorohydrin, isocyanates, or styrene to produce the final product.

Owing to the high selling price and growing market sizes, fiber-reinforced plastics (FRPs) are also ideal applications in which to use renewably sourced, bio-based monomers.[37] Typically, FRPs are used for applications that require high strength (afforded by the combination of polymer properties and fiber reinforcement) and exhibit light-weight and long lifetimes, such as wind turbines, automotive parts, and high-performance sporting equipment. Meanwhile, bio-based monomers derived from lignocellulosic biomass afford additional functionality or properties

[1]National Bioenergy Center, National Renewable Energy Laboratory, Golden, CO 80401, USA

[2]Strategic Energy Analysis Center, National Renewable Energy Laboratory, Golden, CO 80401, USA

[3]Lead Contact

*Correspondence: gregg.beckham@nrel.gov

https://doi.org/10.1016/j.joule.2019.01.018

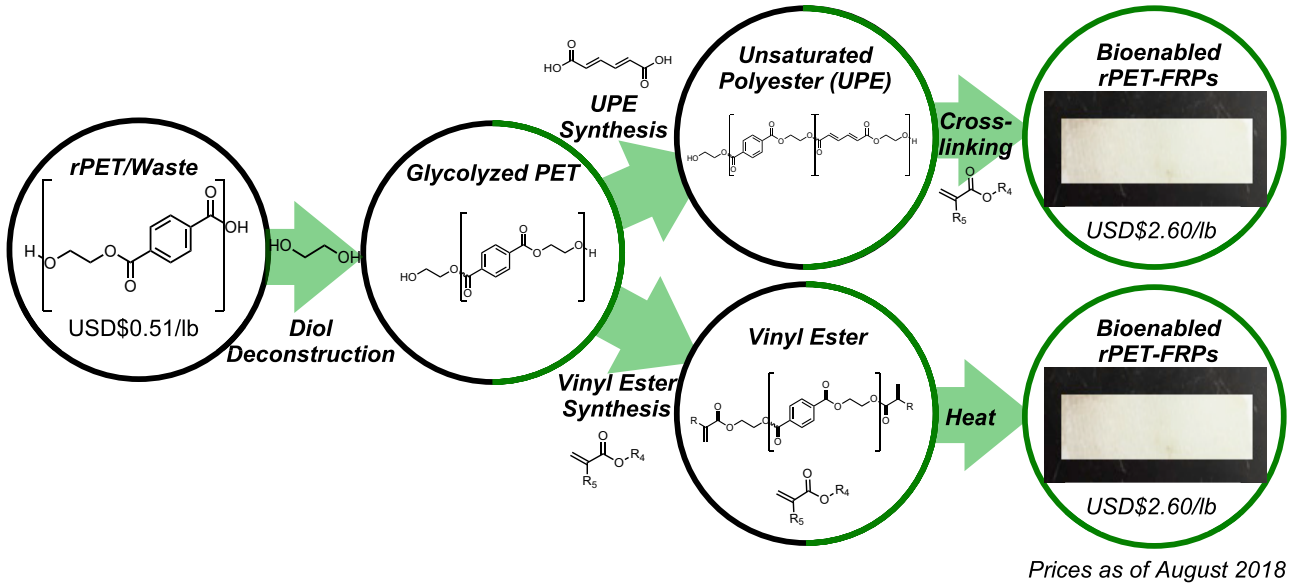

Scheme 1. Overview of This Work in which rPET, a Low-Value Material, Is Converted to Higher-Value FRPs through Two Routes

In both routes, rPET is initially glycolyzed with diols, which can be renewably sourced and subsequently converted into a UPE or vinyl esters with renewably sourceable monomers. Subsequently, both polymer backbones are dissolved in a renewably sourceable reactive diluent and applied to a fiberglass mat to produce an FRP.

owing to their high oxygen content and chemical characteristics not typically or readily available in monomers derived from petroleum routes. Previous work on synthesizing FRPs from biomass[38] implemented the dimethyl isomers of muconic acid into the backbone of poly(butylene succinate) (PBS). Once methods were developed to ensure stoichiometric incorporation of the muconic acid isomers into PBS,[39] FRPs with the isomers of muconic acid, fumarate, and maleic anhydride were synthesized. The final properties of the FRPs demonstrated that the functionality imparted by muconic two carbon-carbon double bonds in muconic acid results in materials with superior properties to those derived from maleic anhydride, a common petroleum-derived olefinic monomer with only one carbon-carbon double bond.

In this work, reclaimed PET (rPET) and renewably sourceable monomers are combined to produce high-value FRPs. To accomplish this, PET was first deconstructed and glycolized with linear diols that can be obtained from renewable sources and subsequently reacted with renewably sourceable monomers to produce a series of UPEs or diacrylic polymers. These polymers were then dissolved in a reactive diluent with a free radical initiator to form a resin, which is applied to a woven fiberglass mat and reacted to produce a series of rPET-FRPs (Scheme 1). In all cases presented here, rPET-FRPs produced with renewably sourceable monomers outperform the standard petroleum-based styrene and maleic anhydride. Additionally, acrylic and methacrylic acid, both derivable from bio-based sources, outperform styrene as reactive diluents in nearly every case, as they ensure compatibility between the reactive diluent and polymer. The molecular weight of the PET bottles may exceed 50,000 (5.0×10^4) g/mol (such as those used in this study), and whenever the PET is deconstructed to near 30,000 g/mol, exceptional performance is obtained in the final FRP. Ultimately, this approach could incentivize PET reclamation and lead to reduced plastic pollution while advancing many global sustainability goals by combining biomass with reclaimed plastics.[40]

RESULTS

PET Deconstruction via Glycolization

In this study, rPET from single-use, carbonated beverage bottles were the primary source of PET. rPET was procured locally and cut up into fine strips after removing the labels and cap. To be used in a UPE, the rPET was initially depolymerized to a lower molecular weight via transesterification in the presence of a diol and a catalyst. Ethylene glycol or 1,4-butanediol were used as the diol, and titanium butoxide was used as the catalyst. Table 1 presents the molecular weight of the deconstructed rPET as a function of reactor loading of ethylene glycol or butanediol. As the diol loading increases, the rPET molecular weight is reduced, as expected. The use of excess diol ensures that the rPET becomes hydroxyl-terminated, enabling all subsequent chemistries. When butanediol is used as the deconstruction solvent instead of ethylene glycol, minimal differences are observed. Hydroxyl termination is associated with the use of titanium butoxide as a catalyst, which promotes transesterification. However, as there is a lower molar quantity of butanediol (at the same mass loading of ethylene glycol), the molecular weight of the deconstructed rPET is slightly higher. These reaction conditions were selected because of literature precedence;[20] it should be noted that glycolysis optimization is not the focus of this study. Unless otherwise noted in the following sections, the rPET used in the backbone of the UPEs and vinyl ester data is the deconstructed rPET from clear bottles using ethylene glycol with a molecular weight of 1.5×10^4 g/mol (EG:PET mass ratio of 2:1).

FRPs from Unsaturated Polyesters

After the PET was deconstructed (and, effectively, all chain ends were modified to alcohols), malate, fumarate, and the *cis*,*cis* and *trans*,*trans* isomers of dimethyl muconate were incorporated via melt blending with the same transesterification catalyst to synthesize UPEs (Scheme 2). NMR spectroscopy of the resultant rPET-UPE indicates that all monomers were incorporated stoichiometrically into the polymer backbone without side reactions (Figures S1–S5), and gel permeation chromatography (GPC) (Figure S6) indicates that homopolymers were formed. A series of rPET-FRPs were synthesized by dissolving the UPE in a reactive diluent (i.e., styrene, methacrylic acid, or acrylic acid) with a free radical initiator (azobisisobutyronitrile, AIBN) to form a resin and then applying the resin to a fiberglass mat.

The storage and loss moduli of the FRPs depend on the olefinic diacid used, the loading of the diacid, and the compatibility of the reactive diluent, as demonstrated in Figure 1 for styrene as the reactive diluent. In general, higher storage moduli are favored for higher material strengths, while lower loss moduli are favorable as they indicate a better adhesion to the fiberglass mat. At lower loadings, there is compatibility between the styrene and the UPE, which arises due to the olefinic block randomly disrupting any crystalline domains. However, at higher loadings (where larger regions of the olefinic block can occur), there is a large degree of incompatibility between styrene and the UPE, leading to poor FRP performance as indicated by lower storage moduli and higher loss moduli.

When a renewably sourceable, reactive diluent is used, specifically an acrylic carboxylic acid (in this study methacrylic or acrylic acid), there is compatibility between the UPE and the reactive diluent, resulting in consistent FRP properties, as demonstrated in Figure 2. At lower olefinic acid loadings in the UPE backbone, the styrene-based FRPs slightly outperform the acrylic-acid-based UPEs in terms of the storage modulus. However, in terms of loss moduli, the methacrylic- and acrylic-acid-based FRPs outperform the analogous styrene-based systems. Differences between methacrylic acid and acrylic acid are minimal in the case of FRPs

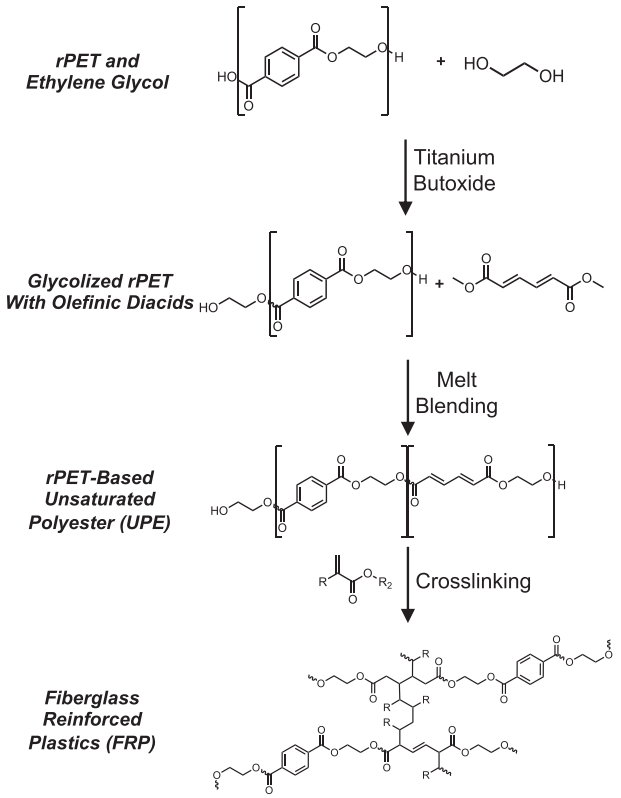

Scheme 2. The PET Deconstruction, UPE Synthesis, and FRP Synthesis Scheme Employed in This Work

PET is partially depolymerized with titanium butoxide in excess ethylene glycol, melt blended with olefinic acids, and subsequently converted into an FRP. Scheme S1 provides the petroleum base case used for comparison.

synthesized from UPEs. Additionally, when there is compatibility between the polymer and reactive diluent, the extent of crosslinking is higher, which is observed in the near-quantitative mass balance for the successful FRPs (Table S3). This series of FRPs

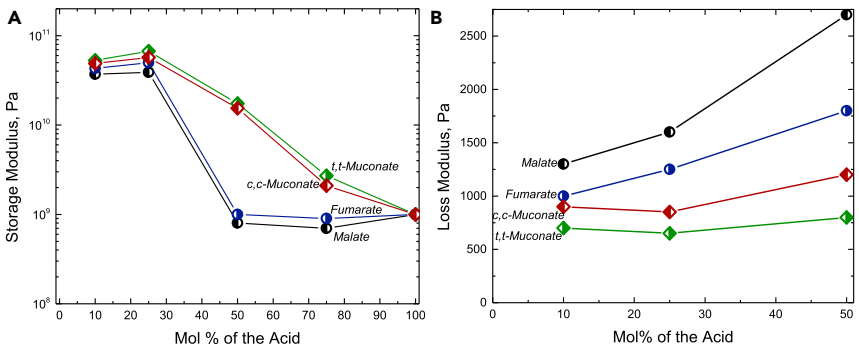

Figure 1. Storage and Loss Moduli of FRPs with Styrene as a Reactive Diluent

(A) Storage moduli and (B) loss moduli at 35°C as a function of olefinic acid loading for the rPET-FRPs with styrene as the reactive diluent. At low loadings of the olefinic acid, there is compatibility with the styrene; however, there is no compatibility at higher loadings. In all cases, the muconic acid isomers outperform fumaric acid (with *trans,trans* muconate outperforming the *cis,cis* isomer). In turn, fumaric acid outperforms maleic anhydride. Data are represented as the mean ± SD, and the SD is less than the symbol size.

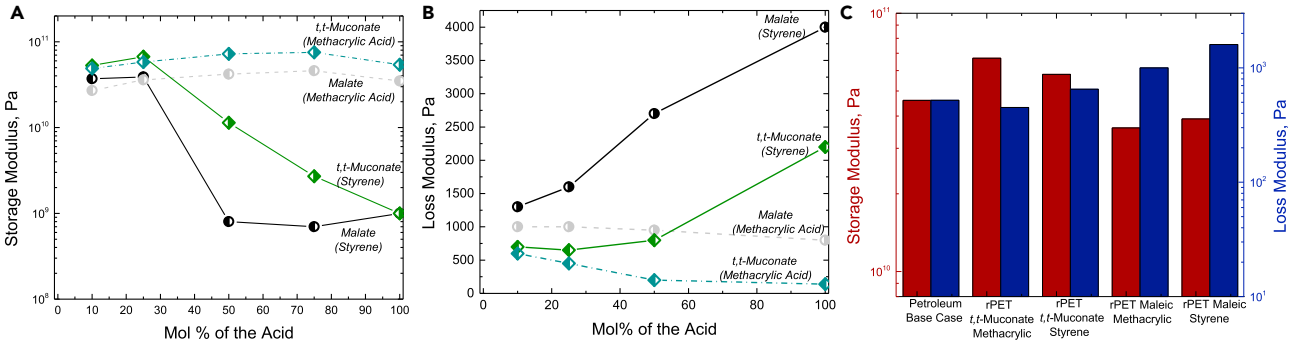

Figure 2. Storage and Loss Moduli of FRPs Comparing Styrene and Methacrylic Acid as Reactive Diluents

(A and B) A comparison of (A) storage moduli and (B) loss moduli at 35°C as a function of olefinic acid loading for the rPET-based FRPs with styrene (solid lines) and methacrylic acid (dotted lines) as the reactive diluent. The olefinic carboxylic acids demonstrate compatibility with the UPEs across the entire property range, thus resulting in robust FRPs with muconic acid outperforming maleic anhydride.

(C) When compared to a petroleum formulation of isophthalic acid, 1,2-propanediol, and 25 mol % maleic anhydride, the rPET-FRPs that implement methacrylic acid (or acrylic acid) outperform in both the storage and loss moduli. Reaction scheme for the petroleum base case is provided in Scheme S1. Additionally, Figure S7 provides the frequency dependence graphs for the 50% loading cases demonstrating that as UPE and reactive diluent compatibility decreases, frequency dependence behavior emerges.

For (A) and (B), data are represented as the mean ± SD, and the SD is less than the symbol size. For (C), error bars are not presented because of the log scale.

was also compared to a petroleum-based FRP. For the base case, the UPE was synthesized from 1,2-propanediol, isophthalic acid, and maleic anhydride at a molar ratio of 1:0.75:0.25 and comparable molecular weight.[41] Subsequently, the UPE was dissolved in styrene, and the FRP was synthesized. When compared to the rPET-FRPs in this study (Figure 2C), the petroleum base case outperforms the rPET-FRPs that use maleic anhydride in their backbone. However, the FRP composed of renewably sourceable muconic acid and rPET, specifically PET-co-25 mol %-*trans*,*trans*-muconate (rPET-25-*tt*M), outperforms the petroleum base case.

The FRP performance as a function of starting rPET molecular weight was also investigated. Figure 3 provides the storage and loss moduli as a function of molecular weight (a measure of the extent of PET deconstruction) for a representative PET-co-50 mol %-*trans*,*trans*-muconate (rPET-50-*tt*M) FRP with methacrylic acid as the reactive diluent. At lower levels of rPET deconstruction (and thus higher UPE molecular weights), the moduli are strongly dependent on the UPE molecular weight due to the poor solubility of the UPE in the reactive diluent. At higher degrees of deconstruction (lower UPE molecular weight), there is little dependence because the UPE is soluble in the reactive diluent and excellent material properties (storage and loss moduli) are obtained. At lower molecular weights, the constant storage and loss moduli are associated with the olefinic moieties being randomly distributed through the backbone of the UPE, which results in a constant molecular weight between crosslinks.

FRPs from Diacrylic Polymers

Diacrylic polymers were also prepared in place of the UPE as outlined in Scheme 3 in which 60 wt % deconstructed rPET was added to a reactor with 40 wt % olefinic carboxylic acid, either methacrylic or acrylic acid. The benefit of this method is that, after polymerization, a free radical initiator can be added to the reaction mixture and then directly aliquoted to the fiberglass mat for immediate FRP synthesis. To compare the performance of the diacrylic polymers to that of a petroleum-derived alternative, the olefinic monomer was removed via vacuum distillation and the diacrylic polymer subsequently dissolved in styrene.

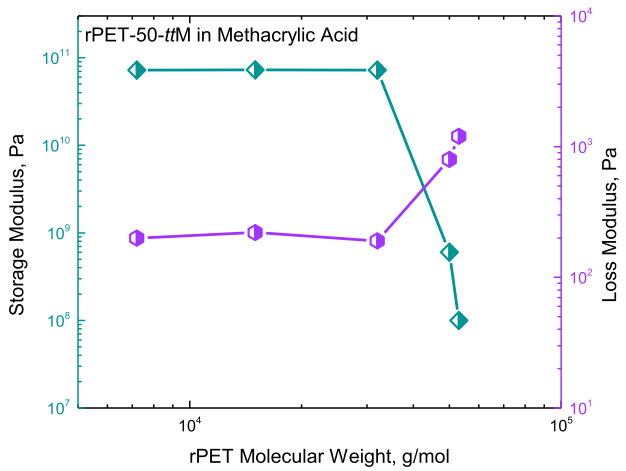

Figure 3. Storage and Loss Moduli at 35°C for the rPET-50-*tt*M FRPs with Methacrylic Acid as the Reactive Diluent as a Function of rPET Molecular Weight

At higher molecular weights (lower mass ratio of EG to PET), the rPET-UPEs are not soluble in the reactive diluent. However, at lower molecular weights, there is no dependence between molecular weight and deconstruction. When using UPEs in the polymer backbone, differences between methacrylic and acrylic acid are negligible. Data are represented as the mean ± SD, and the SD is less than the symbol size.

The FRPs from the diacrylic polymers exhibit the same exceptional performance as UPEs derived from renewably sourceable resin (Figure 4). In all diacrylic polymer cases, styrene possesses poor compatibility and poor performance (Figure S10). In some cases, the FRPs from the diacrylic polymers exhibit higher moduli and lower loss moduli than the UPEs. However, unlike the UPEs, the diacrylic polymers exhibit a slight molecular weight dependence across the range used in this study. This behavior is explained by the fact that the only reaction sites for the diacrylic polymers are at their chain ends. As the molecular weight between the crosslinks scales inversely with shear and storage moduli, changing the molecular weight of the starting PET material has an effect on the moduli. The dotted lines parallel to the x axis indicate a BHET control, taken to be the upper limit of the rPET-FRP properties.

Thermal Properties

All FRPs in this study maintained favorable thermal properties, specifically their glass transition temperature, T_g, as long as the reactive diluent was compatible with the polymer backbone. In the case of FRPs, the T_g is an indication of the maximum temperature up to which it can be used and maintain consistent mechanical properties. Figure 5 presents the T_g values for representative FRPs produced in this study. When the styrene is compatible with the UPE, the FRPs exhibit exceptional T_g (~90°C); however, when the styrene is incompatible with the UPE, the FRP exhibits a lower mass balance (Table S3) and, effectively, a lower degree of crosslinking that leads to the reduction in T_g because of a less-robust network. As all FRPs prepared with the renewably sourceable reactive diluents exhibited compatibility with the olefinic polymers, they all exhibit high T_g values.

Comparison to Virgin PET, Green rPET, and Butanediol-Deconstructed PET

To assess if contaminants (e.g., the residual bottle label) made it into the final FRP, in-house synthesized or virgin PET at a comparable molecular weight to the rPET (Table 1) was used to manufacture a series of control FRPs. This virgin PET sample was used to synthesize a series of polymers, specifically a 50% loading *trans,trans*-muconic acid UPE, a 50% loading maleic anhydride UPE, a methacrylic diacrylic

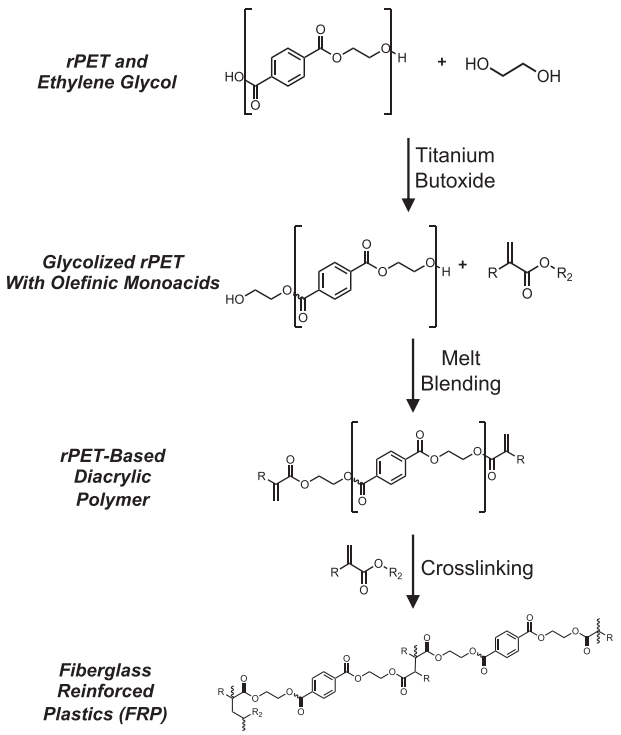

Scheme 3. The PET Deconstruction, Diacrylic Synthesis, and FRP Synthesis Approach Employed in This Work

PET is recycled with ethylene glycol, blended with olefinic mono-acids, and subsequently converted into an FRP. In the diacrylic polymer-vinyl ester synthesis, there is no need for separations following reaction with the acrylic acid. Scheme S1 provides the petroleum base case used for comparison. Figures S8 and S9 provide the NMR for these polymers, while Table S2 provides the GPC results.

polymer, and an acrylic diacrylic polymer at a molecular weight of ~15,000 g/mol. The UPEs and diacrylic polymers were subsequently reacted with the three different reactive diluents with the fiberglass mat to produce FRPs. Figure 6 shows the storage moduli for these FRPs. The differences between the virgin PET and the rPET are minimal. When styrene is used as the reactive diluent, the FRPs possess low storage moduli owing to poor compatibility with the styrene. When either acrylic or methacrylic acid is used as the reactive diluent, the FRPs derived from virgin PET and rPET exhibit comparable performance. At this molecular weight, the diacrylic polymers slightly outperform the UPE. The same series of FRPs was also synthesized using green-colored rPET bottles to assess the effect of the coloring on material properties (Figure 6B). The green tinted bottles resulted in no adverse effects in the storage moduli or loss moduli of the final product. Additionally, because of the glycolization procedure used in this work, any color was washed away, and the final product appeared white by eye (Figure S12). Finally, the same series of polymer backbones were synthesized from the butanediol-deconstructed rPET at the same 2:1 diol-to-PET loading, and negligible differences were observed here as well (Figure 6C).

Cradle-to-Gate Analysis of rPET-FRPs from UPE

To assess the energy savings potential of the proposed FRP production method from rPET and bioderived monomers, the Materials Flows through Industry (MFI) supply chain analysis tool[42] was used. MFI models the supply chain of a commodity as a network of unit processes covering natural resource extraction through to the final

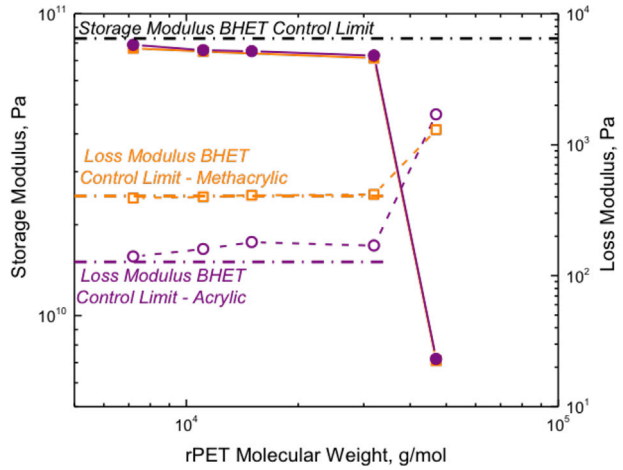

Figure 4. Storage and Loss Moduli of the Diacrylic Polymers as a Function of Molecular Weight
Storage (solid symbols – left axis) and loss (open symbols – right axis) moduli for the rPET-diacrylic FRPs as a function of molecular weight for both the acrylic (purple circles) and methacrylic (orange squares) FRPs. Differences between the acrylic and methacrylic systems manifest in the loss modulus. The black dashed line indicates the storage modulus for the acrylic and methacrylic monomers synthesized with a BHET control. Data are represented as the mean ± SD, and the SD is less than the symbol size.

production step. The "supply chain energy" calculated by MFI is therefore the sum of all energy inputs required by this set of unit processes and includes processing fuel, electricity, transportation energy, and energy contained in fossil chemical feedstocks. Similarly, greenhouse gas (GHG) emissions are totaled for all combustion processes within the supply chain, including process heating, electricity generation, and transportation of inputs. The tool calculates direct displacement offsets for production of coproducts and byproducts in these supply chains, presenting results on a net basis. For electricity requirements, the 2016 US grid mix is assumed.[43]

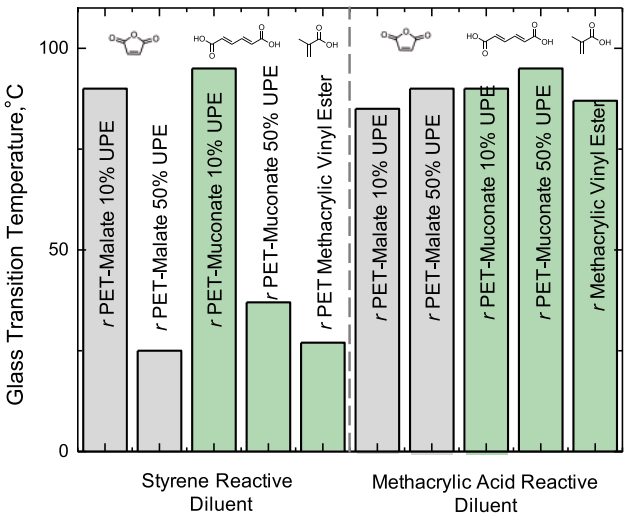

Figure 5. Glass Transition Temperature, T_g, for the Various FRPs Synthesized in This Study
When the rPET-polymers are incompatible with styrene, the overall FRP is plasticized and exhibits a low T_g, which contributes to poor mechanical performance. When a compatible reactive diluent is used, all rPET-FRPs exhibit high-non-plasticized (>85°C) T_g values. Digital scanning calorimetry (DSC) traces are provided in Figure S11. The SD in the data is ± 3°C across the entire dataset.

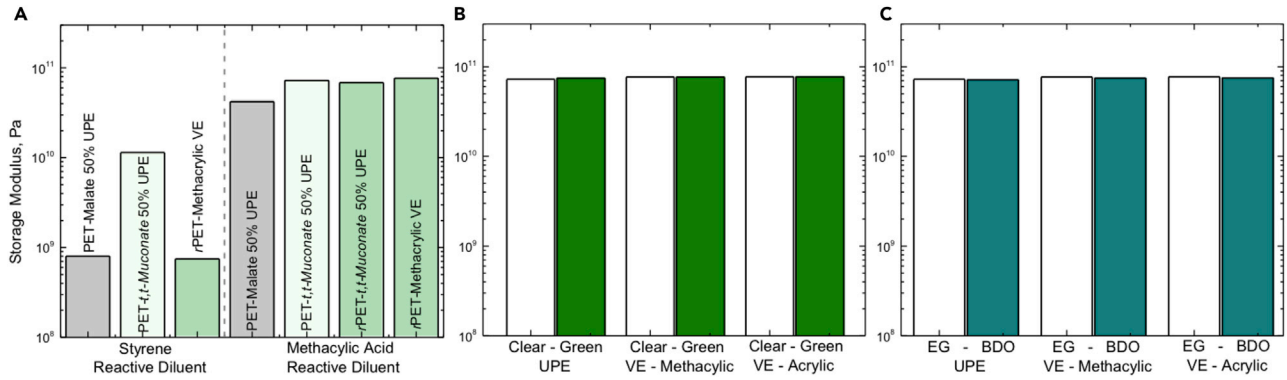

Figure 6. Comparison of FRPs between Different Sources of PET

Storage moduli for the case studies of (A) virgin PET, (B) green rPET, and (C) butanediol glycolyzed rPET. FRP property differences due to these changes are minimal. Pictures of an FRP from a clear and a green bottle are provided in Figure S2. Error bars are not presented because of the log scale, and the SD is within 5% of the mean value.

In cases where supply chain inputs are manufactured using multiple technologies (i.e., production routes), the requisite unit processes are weighted to reflect current US industry practices. All other assumptions of the MFI tool, such as sector transportation assumptions, are discussed in more detail in work by Hanes and Carpenter.[42]

To compare the laboratory-scale methods presented in this work with industrial FRP manufacturing, a scale-up method presented by Piccinno et al. was implemented.[44] As the laboratory scale may not correspond to industrial practice, the Piccinno et al. method provides a conservative comparison by overestimating the energy requirements, often including extra steps that may not be industrially relevant. One such included step in the analysis and the bench scale was the vacuum drying of the UPE prior to dissolution in the reactive diluent step between polymerization and UPE manufacture. Additionally, the supply chain energy and GHG calculations for the rPET-FRPs were calculated via two approaches, a waste valuation estimation approach and a cutoff approach.[45] The waste valuation estimation approach accounts for the commercial value of the rPET material. An environmental burden from the original bottle production (energy and GHGs in this analysis) is assigned to the rPET determined by the ratio of the market price of rPET relative to the market price of virgin PET. Conversely, the cutoff approach assumes that the rPET is a waste product with no value and therefore is not assigned any of the environmental burdens from virgin PET bottle production.

In total, five cases were studied and are listed in Table 2 and Figure S13. In the base case, an FRP synthesized from styrene and a UPE with a composition of 37.5 mol % isophthalic acid, 50 mol % propylene glycol, and 12.5 mol % maleic anhydride was used. In the other four cases, a UPE composition of 37.5 mol % terephthalic acid, 50 mol % ethylene glycol, and 12.5 mol % muconic acid was used. These FRPs correspond to the FRPs presented in Figure 3C. In the case of the waste-valuation method, clear and green-colored recycled PET have different market prices, hence the two different estimations. Additionally, estimates for the energetic demand of muconic acid and acrylic acid were based on the use of lignocellulosic sugars from second-generation corn-stover biomass (C.W. Johnson, D. Salvachúa, N.A.R., B.A. Black, D.R. Vardon, P. St. John, G.T.B., and M.J.B., unpublished data).[46] In the case of butanediol, the process implemented by Genomatica for the direct fermentation of first-generation sugars and subsequent separation of butanediol was

Table 2. MFI Case Study Description

Case Study Name	Description
Petroleum base case	base case in which the reactive diluent is styrene and the UPE is a mixture of propanediol, isophthalic acid, and maleic anhydride
Economic waste valuation, clear bottle	a waste valuation estimation using bioderived muconic at a loading of 25% and acrylic acid combined with a clear PET bottle deconstructed with petroleum-derived ethylene glycol at a mass ratio of 2:1
Economic waste valuation, green bottle	a waste valuation estimation using bioderived muconic at a loading of 25% and acrylic acid combined with green-colored PET bottle deconstructed with petroleum-derived ethylene glycol at a mass ratio of 2:1
Cutoff rPET, petroleum acrylic acid	cutoff rPET estimation using bioderived muconic at a loading of 25% and petroleum-derived acrylic acid; the PET was deconstructed with petroleum-derived ethylene glycol at a mass ratio of 2:1
Cutoff rPET, bioderived acrylic acid	cutoff rPET estimation using bioderived muconic at a loading of 25% and bioderived-derived acrylic acid; the PET was deconstructed with petroleum-derived ethylene glycol at a mass ratio of 2:1

Molecular weight error is ±0.2. The polymer produced at a mass ratio of 2.0 was the base polymer for most subsequent experiments. In molar equivalents, the amount of ethylene glycol ranges from approximately 0.5 to 8.

implemented,[47] while the bioderived ethylene glycol models were based on the conversion of bioderived ethylene as an illustrative example.

As presented in Figure 7A, the supply chain energy for the petroleum-derived FRP is approximately 88 MJ/kg, and in all rPET cases, the supply chain energy is lower. The waste valuation scenarios yield supply chain energies of 56 and 49 MJ/kg, for the clear and green-colored rPET-based FRPs, while the zero-value PET results in supply chain energies of 45 and 37 MJ/kg for the petroleum and bioderived acrylic acid rPET-based FRPs. Overall, these represent 36%, 45%, 49%, and 57% potential savings in supply chain energy, respectively. The majority of the potential reduction in supply chain energy requirements is due to the reduction in fossil feedstock energy and, to a lesser extent, reductions in process fuel (e.g., natural gas for heating applications). Figure 7B also provides an estimate of the energy content of fossil feedstocks (coal, crude oil, and natural gas) consumed in the supply chain for non-combustion applications (i.e., conversion to precursor chemicals). The base case requires 39 MJ/kg of this feedstock energy (most of which is contained in crude oil),

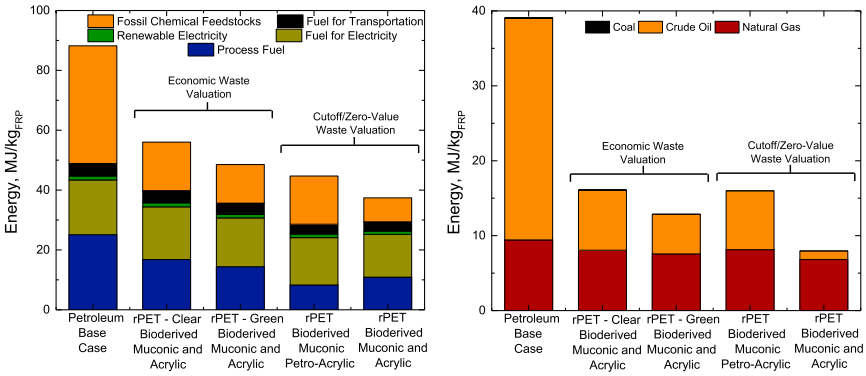

Figure 7. Supply Chain Energies for the Different Case Studies

Supply chain energy results from the MFI tool for (A) the total supply chain and (B) the fossil chemical feedstock energy associated with the FRP process implementing UPEs. The numerical breakdown is provided in Tables S4 and S5.

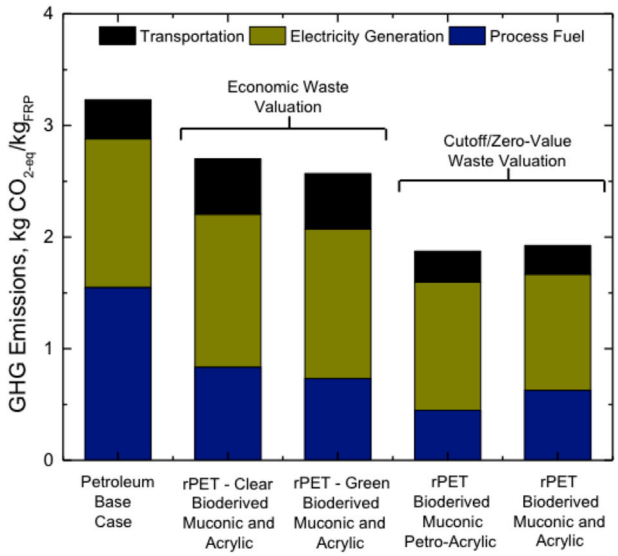

Figure 8. GHG Emissions in kg $CO_{2\text{-}eq}$/kg_{FRP} for Each of the Five Cases

while the four rPET specifications require 16, 13, 16, and 8 MJ/kg of feedstock energy, respectively. These represent 59%, 67%, 59%, and 80% potential savings in feedstock energy, respectively.

In addition to the supply chain energies, the MFI tool also calculates GHGs in terms of kilograms of carbon dioxide equivalent per kilogram of product (kg-$CO_{2\text{-}eq}$/kg_{FRP}). Supply chain GHG estimates are presented in Figure 8. The base case FRP requires 3.23 kg-$CO_{2\text{-}eq}$/kg_{FRP}, while the other four cases require 2.26, 2.13, 1.87, and 1.94 kg $CO_{2\text{-}eq}$/kg_{FRP} and represent savings of 30%, 34%, 42%, and 40%, respectively. Using petroleum-based acrylic acid leads to slightly lower supply chain GHG emissions because of the slightly higher process fuel and electricity requirements in the modeled bio-based acrylic acid supply chain.

The Supplemental Information provides sensitivity analysis for excluding a drying step (Table S6), implementing different ethylene glycol loadings in the deconstruction of PET (Tables S7 and S8), using a lower muconic acid loading level (Table S9), sourcing muconic acid from first-generation commodity sugars instead of second-generation lignocellulosic sugars (Table S10), implementing petroleum-derived butanediol (Table S11), and implementing bioderived butanediol from commodity sugars (Table S12) and bioderived ethylene glycol from bioderived ethylene (which comes from the dehydration of bioderived ethanol) (Table S13).[48] Overall, two sensitivity cases stand out as the largest potential source of supply chain energy and emissions variation: the amount of ethylene glycol used in deconstruction or the use of butanediol (petroleum and biomass derived). The use of second-generation feedstocks for muconic acid has a modest effect. Changing the loading of muconic acid and omitting the vacuum drying step both appear to have a negligible effect on the calculated supply chain energy and GHG emissions.

DISCUSSION

This work aims to combine bio-based building blocks with rPET to produce high-value composite materials that could serve to both incentivize the bioeconomy and foster a greater plastics recycling or upcycling mentality. As of August 2018, rPET is estimated to sell for approximately $0.51 USD/lb for clear PET flake and

0.31 $USD/lb for green-colored PET flake, while virgin PET is estimated to sell for $0.82 USD/lb.[49] To provide an incentive for rPET reclamation, it is necessary to find markets with higher-value products and demonstrate performance differentiation from petroleum-based standard materials. One such application space that demands a higher selling price is the UPE resins market, which sells at approximately $2.60 USD/lb.[50] UPE resins are versatile materials used in many applications across multiple economic sectors and possess a growing global market forecast that is expected to reach $10.48 billion USD in 2019.[36,51] Additionally, UPE resins produced from rPET and renewably sourced monomers may exhibit lower energy intensity and GHG emissions on a cradle-to-gate, supply chain level than their petroleum-derived counterparts.

FRPs are made of two components: a fiberglass mat and a resin. Typically, the resin is composed primarily of a polymer backbone (e.g., a UPE), a reactive diluent, and other small processing additives. As presented in this work, the effect of the reactive diluent on the mechanical properties is significant. Styrene is the most widely employed reactive diluent owing to its cost, favorable reactivity, and the robust thermal and mechanical properties when polymerized.[52] Typical industrial practice is to tailor the UPE to fit the need of the reactive diluent. Despite the widespread use of styrene, it is a carcinogen with high vapor pressure.[53] As a note, for this study, styrene is not considered to be a renewably sourceable monomer; however, styrene can be produced biologically and this is an active area of research.[54–56]

In the present work, methacrylic acid and acrylic acid were used as reactive diluents to enable the use of the rPET-polymer backbones in the FRPs and to improve material properties. Methacrylic acid can be produced via decarboxylation of itaconic acid,[57,58] which can be obtained biologically in high yields.[59–61] Acrylic acid, which is prepared from propylene industrially, can be renewably sourced from a variety of 3-hydoxypropyl functionalized monomers (e.g., 3-hydroxypropionic acid [3-HP] and 3-hydroxypropionaldehyde, etc.) or lactic acid via dehydration.[62–64] Methacrylic acid and acrylic acid both possess lower volatility[65] than styrene and can be modified to further reduce volatility, impart higher strength, or promote adhesion.[66–68] Beyond the present work, there is a wide slate of olefinic monomers that can be obtained from lignin deconstruction.[69] These monomers resemble substituted methylstyrenes and eugenols and might require further reaction development or modification.[70–79] In all cases, as new pathways to styrenic monomers from biomass become prevalent, the methodology in this work can be expanded to renewably sourceable precursors that may possess lower volatility and toxicity. This methodology has already been explored briefly in previous work in which cinnaminic acid was implemented to increase the storage modulus in other FRP systems.[38]

The use of alternative reactive diluents also enables a wider range of polymer backbones (UPEs or the diacrylic polymers) to be implemented. The polymer backbone itself comprises ~60 wt % of the resin mixture, and in current industrial practice, the polymer backbone is typically a UPE synthesized from an olefinic diacid (typically maleic anhydride or maleic acid), a diol (typically propanediol), and a rigid diacid (typically isophthalic acid). In these formulations, the olefinic acid accounts for 10–30 wt % of the polymer backbone,[80,81] while the diol and rigid diacid mixture comprise a majority of the remaining weight. rPET is the ideal replacement for the remainder of the polymer backbone as it is a rigid aromatic diacid (terephthalic acid) and a diol (ethylene glycol). It should be noted that it is also possible to obtain ethylene glycol and terephthalic acid via renewable feedstocks. Ethylene glycol can be produced biologically,[82–85] and terephthalic acid can be produced via the catalytic upgrading of renewable para-xylene (a method

similar to what is employed industrially)[86] or by the Diels-Alder reaction of *trans*,*trans* muconic acid with ethylene followed by dehydrogenation.[87–91] However, the aim of the present work is to enable further PET reclamation.

As demonstrated here and in other work,[32,33] PET cannot be used directly and must undergo modifications prior to UPE synthesis and FRP implementation. Accordingly, when styrene is used as a reactive diluent, the PET must be deconstructed with non-linear diols to ensure compatibility with the styrene.[34,35,66,80] The present strategy enables minimal deconstruction of the polymer to lower molecular weights for use in FRPs, with the key component to rPET implementation being the use of a compatible reactive diluent and substantial breakdown. The diols that can be implemented with no adverse effect on properties are not limited to ethylene glycol and could include renewably sourced diols, such as butanediol. The source of the diols, like butanediol, can be directly from fermentation or from the catalytic upgrading of diacids[92–94] and sugars.[95,96] Even though no stark differences were observed with butanediol as the glycolysis agent, more rigid diols such as isosorbide[97] may impart further property modifications. However, as the suite of diols is changed, deconstruction conditions may also be altered. These studies will be pursued in future investigations.

The final prominent component in the FRP formulation is the olefinic diacid in the polymer backbone. In this work, the olefinic diacids that can be derived from biomass are fumaric, *cis*,*cis*-muconic, and *trans*,*trans*-muconic acid. Fumaric acid can be produced at high titers from both commodity first-generation sugars as well as lignocellulosic sugars.[98–100] *Cis*,*cis* muconic acid can be obtained both via the biological conversion of sugars and aromatic compounds directly or catalytically,[101,102] and *trans*,*trans*-muconic acid can be obtained from the isomerization of *cis*,*cis*-muconic acid.[87,103,89,91] In the case of fumaric acid, its *trans* configuration (relative to maleic acid's and anhydride's *cis* configuration) enables higher reactivities and thus better properties at the same cure time,[38,104] while the two double bonds in muconic acid enable additional rigidity and a higher degree of crosslinking. Beyond the present work, olefinic diacids, such as itaconic acid, have already been implemented in UPEs.[105] The diverse functionality inherent to bioderived monomers can enable future modifications that impart tunable properties (e.g., improved rigidity from ketones, adhesive properties from side chain functionality, etc.). Even though it is beyond the scope of the present study, the higher storage moduli and adhesions to the fiberglass mats may enable longer lifetimes, warranting further study of renewably sourceable monomers for FRP applications. In general, the lifetime of FRPs can vary widely depending on their final application and are typically incinerated or landfilled at the end of life. Further research will investigate other end-of-life applications for current FRPs and more sustainable chemistries for future FRP formulations.

The benefit of this methodology is not limited to the utilization of biological or low-value PET streams but also may lead to a lowering of the energy consumption and GHG emissions associated with composites manufacturing. Numerous studies on the energetic demands of PET recycling[45,106–110] have demonstrated that the use of rPET via mechanical or chemical recycling methods may exhibit lower GHG emissions and energy requirements compared to virgin PET manufacture. These estimates vary widely depending on the study (by up to 100%), and there are no current complete studies to our knowledge that investigate the recycling of PET using bioderived monomers. In this work, we show that the supply chain energy required to produce FRPs from rPET and biomass-derived monomers is potentially lower than

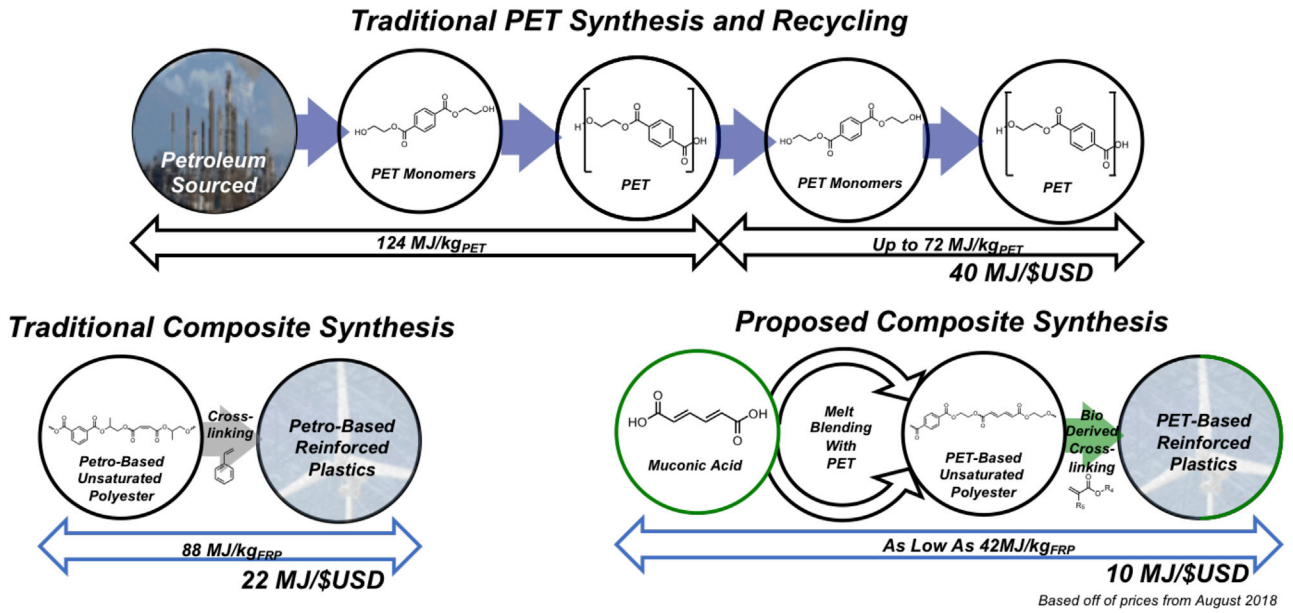

Figure 9. Supply Chain Energy Calculated Using the MFI Tool for the Manufacture of 1 kg of Resin

For traditional PET synthesis, values are per kilogram of PET produced, and for the composite synthesis, the results are per kilogram of final FRP. Potential supply chain energy per dollar is calculated by comparing to prices as of August 2018.

that of both chemically recycling PET back to bottle-grade PET and the conventional fossil-based FRP production process, as summarized in Figure 9.

The manufacture of virgin polymers from petroleum feedstocks is an energy-intensive process, with most polymers requiring 90–200 MJ/kg. The MFI tool estimates that the virgin PET production supply chain requires 124 MJ/kg. Meanwhile, the MFI tool predicts that the current fossil-based FRP supply chain requires 89 MJ/kg. The lower associated energy of homopolymer manufacture (such as PET) and FRP manufacture is the result of the reactive diluent lowering the manufacturing intensity. If the glycolization procedure from this work is applied to chemically recycle the PET in a bottle-to-bottle fashion (using ethylene glycol in a 4:1 mass ratio relative to the PET), the associated energy in the manufacture of a "new" bottle is 72 MJ/kg$_{PET}$ (Table S13). Meanwhile, the method presented herein of producing FRPs from rPET and biomass-derived monomers exhibits substantially lower supply chain energy requirements of 37–56 MJ/kg and potential supply chain GHG emissions savings of 0.9–1.3 kg$_{CO2\text{-}eq}$/kg$_{FRP}$. If this technology were used to manufacture the roughly 740,000 metric tons of FRP produced in the US annually,[111] GHG offsets could range from 0.7 MMT-$CO_{2\text{-}eq}$ to 1.0 MMT-$CO_{2\text{-}eq}$ per year, which is equivalent to emissions of between 150,000 and 200,000 cars, assuming a factor of 4.67 metric tons CO_2e/vehicle/year as calculated by the United States Environmental Protection Agency (EPA). This production would use less than 10% of the total PET-single-use bottle stream and less than 50% of the recycled PET. Additionally, FRPs have a higher selling price ($1.85 USD/lb)[50] than PET resin ($0.81 USD/lb).[49] These differing prices are combined with the estimated per-kilogram supply chain energy requirements for the two materials to determine an economic intensity metric in energy-per-dollar units. Such a metric provides a useful comparison of recycling-derived products with differing end uses and goes beyond the energy-per-mass comparison. This study estimates that the rPET-derived FRPs require 10 MJ/$USD of energy compared to the 40 MJ/$USD for recycled bottle-grade

PET resin and 22 MJ/$USD for the virgin FRP. The lower overall intensity in the former is achieved via the use of bioderived resins.

A majority of the supply chain energy in this methodology is attributed to petroleum-derived ethylene glycol. As revealed in the sensitivity analysis, every mass equivalent of petroleum-derived ethylene glycol used in PET glycolization results in an additional supply chain energy of 8 MJ/kg of final FRP product. To demonstrate the effect of a bio-based diol, the effects of bioderived ethylene glycol and butanediol were modeled. For butanediol, the process currently used by Genomatica for the direct fermentation of 1,4-butanediol was modeled. 1,4-butanediol exhibits a higher supply chain energy when compared to ethylene glycol because of the energy (specifically steam) needed for separation and purification. Despite the higher supply chain energy of both bio- and petroleum-based butanediol, the use of a biologically derived source reduces the overall supply chain energy by 10 MJ/kg_{FRP}, mainly owing to a reduction in feedstock energy. In the case of the current technology for bioderived ethylene glycol from bioderived ethylene, a reduction of 3 MJ/kg_{FRP} is predicted. The lower reduction in supply chain energy associated with using bioderived ethylene glycol over bioderived butanediol (3 MJ/kg_{FRP} versus 10 MJ/kg_{FRP}) is associated with the lower atom efficiency of producing ethylene (a C2 carbon) over other products. In this study, the diol used in PET deconstruction has a minimal effect of the mechanical properties of the FRP, which further encourages investigation into and implementation of diols that require the lowest supply chain energy.[47,112,113]

The acrylic acid pathway used in this analysis is based on the dehydration of 3-HP obtained from the low-pH fermentation of sugars from corn stover. Supply chain GHG emissions are slightly higher than in the petroleum-derived acrylic acid case for the scenario modeled with this method of producing acrylic acid, which has not yet been optimized for commercial-scale production. Future improvements to the production of acrylic acid, through either a 3-HP pathway or alternative routes such as lactic acid, might reduce energy requirements and GHG emissions. Improvements in this vein are present in the current work where the use of second-generation muconic acid (derived from the lignocellulosic sugars instead of commodity sugars) in place of first-generation muconic acid (from commodity sugars) results in a 5 MJ/kg_{FRP} reduction in supply chain energy and a 0.2 $kg_{CO2\text{-}eq}/kg_{FRP}$ reduction in net GHG emissions. Further research in the field of fermentation and separation technologies may lead to reductions in both supply chain energy and GHG emissions.

Conclusions

This work demonstrates the ability of renewably sourceable monomers to enable PET to be upcycled into composites, specifically FRPs. In total, this methodology produces FRPs with better mechanical properties that can be produced using a fraction of the energy (on either a monetary or mass basis) when considering the full cradle-to-gate supply chain. The increase in value that PET can undergo when it is upcycled to an FRP not only provides economic incentives for PET reclamation but may enable a potential premium to be charged for the requisite renewably sourceable monomers. Overall, the bio-based monomer upcycling strategy presented in this work may advance many global sustainability goals and could be applied to other high-volume plastics-based materials to further enable the bioeconomy and materials with properties that exceed the petroleum incumbent.

EXPERIMENTAL PROCEDURES

Unless otherwise noted, all materials were purchased from Sigma-Aldrich. Muconic acid was obtained biologically via the fermentation of benzoic acid by *P. putida*

KT2440; more details can be found in the study by Vardon et al.[114] PET was either synthesized from Sigma-Aldrich terephthalic acid and ethylene glycol or reclaimed from local usage. Labels were removed by hand from the rPET bottles, and the bottles were subsequently washed with soap, deionized (DI) water, and acetone to remove any traces of the original contents. Following washing, the PET bottles were cut by hand for immediate use.

PET Deconstruction

PET was deconstructed with butanediol or ethylene glycol. Initially, PET was placed into a round-bottom flask affixed with a condenser. Variable amounts of the diol (Table 1) were loaded into the reactor with 0.5 wt % titanium butoxide, and the reactor was heated up to 220°C. The transesterification reaction proceeded under reflux for 4 h. Following the reaction, the slurry was removed from the reactor and washed with an excess of water to remove unreacted diol and any ethylene glycol that was removed via transesterification. The polymer-water mixture was subsequently filtered, and the solid polymer precipitate was vacuum dried for 24 h to remove excess moisture and diol.

Homopolymer Synthesis

Initially, poly(ethylene terephthalate-co-fumarate), poly(ethylene terephthalate-co-malate), and poly(ethylene terephthalate-*co*-muconate) were synthesized via melt transesterification with rPET bottles. Initially, the reactor (a three-necked round-bottom flask attached with nitrogen, overhead mechanical stirring motor, and Dean-Stark condenser setup) was loaded with a fixed molar ratio of deconstructed PET relative to the diacid, diester, or anhydride and 0.5 wt % titanium butoxide as the transesterification catalyst. The reaction vessel was heated to 180°C, and polymerization was allowed to proceed for 6 h. This prevented the molecular weight growth of the polymer chain while allowing the olefinic monomers to be incorporated into the polymer backbone.

To synthesize the virgin-PET copolymers, the reactor was loaded with 1.1 molar equivalents of diol to 1 molar equivalent of total diacid/diester/anhydride with no transesterification catalyst. The reaction vessel was initially heated to 180°C, and polymerization was allowed to proceed for 1 h. After 1 h, the temperature was increased to 220°C, a vacuum was applied to the system, and the reaction was allowed to proceed for 5 h. This resulted in a polymer with a molecular weight on the order of 3×10^4 g/mol that was used in comparison to the deconstructed PET.

Diacrylic Polymer Synthesis

The reactor was initially loaded with 40 wt % PET and 60 wt % olefinic acid (acrylic or methacrylic acid) and was allowed to reflux for 6 h. Following reflux, AIBN (the free radical initiator) was added to the reaction mixture, which was subsequently aliquoted for direct use in composite synthesis.

FRP Synthesis

Composites were prepared either by preparing a solution of 39.5 wt % olefinic polymer and 59.5 wt % olefinic acid with 1.0 wt % AIBN as an initiator or by mixing the final vinyl ester solution. The reaction mixture was applied to 2-ply Bondo fiberglass mat, placed between two sheets, and allowed to react for 6 h at 80°C. Following the reaction, the fiberglass was placed in a vacuum oven for at least 48 h to allow for any excess monomer to evaporate. Samples were weighed after vacuum drying, and no significant weight loss was observed.

Structural Characterization

Polymer structure was ascertained via a Bruker Avance III HD 400 MHz NMR spectrometer with a 5 mm Broadband Observe (BBO) probe. Quantitative ^{1}H spectra were acquired with a 90° pulse of 14.5 μs and a 30 s recycle delay at room temperature. Deuterated trifluoroacetic acid (99.9% Cambridge Isotope Lab) with 1% w/w tetramethylsilane (TMS) was used as the solvent. Molecular weight was determined via the use of a Wyatt GPC equipped with a Tosoh column, multiangle light scatter, and refractive index (RI) detector. Hexafluoroisopropanol (HFIP) was used as the elution solvent at a flow rate of 0.5 mL/min.

Physical Property Testing

After vacuum drying, the composites were cut into 60 × 12 × 2 mm pieces for mechanical testing. Mechanical tests were performed on a TA Instruments Q800 Dynamic Mechanical Analyzer at 35°C across a range of frequencies from 0.01 to 10 Hz. Thermal characterization was completed by the use of a TA Instruments Q1000 Digital Scanning Calorimeter and a Q500 Thermogravimetric Analyzer using a ramp rate of 10°C/min.

MFI Methodology

A comparison of the energy requirements and GHG emissions for the reference and rPET-based FRP product systems was conducted using the MFI supply chain analysis tool developed at NREL.[42] The MFI tool quantifies the material and energy requirements of commodity supply chains on a cradle-to-gate basis (i.e., from raw material extraction through the end product [e.g., FRP] production). GHG emissions are estimated only for the combustion of fuel for processing, transportation, and electricity generation; non-combustion GHG emissions are excluded. Unit process data for the conventional 60 wt % UPE resin, 40 wt % fiberglass FRP production system were adapted from composite manufacturing data in the US Lifecycle Inventory (LCI).[41] Laboratory scale unit process inventories for the heating, stirring, filtering, and drying steps of the rPET-FRP production process were estimated following Piccinno et al.[44] Inventories for producing bio-based muconic acid and acrylic acid were taken from the literature.[46,115] All other unit processes for upstream inputs that comprise the MFI database are derived from both publicly available literature sources as well as proprietary sources such as the Ecoinvent database and IHS's (Information Handling Service) Process Economics Program.

In the present work, two approaches are used to model energy and emissions for the rPET upcycling scenario. Since this system involves a recycling step, an allocation scheme must be developed to determine how much of the impacts attributed to the first life (i.e., PET bottle production) should be counted toward the second life and product of interest (FRP). Following Shen et al.,[45] two allocation schemes are used in this analysis: "zero-value" (similar to Shen's cutoff) and "waste valuation." In the former, no impact from PET bottle production is attributed to FRP production. While this method appears most favorable from an energy-savings perspective, it fails to account for any value attributed to postconsumer PET, which has a commercial demand for other recycling applications. To account for this, the "waste valuation" approach attributes a fraction of PET bottle production impacts to the upcycled FRP. This fraction is equal to the ratio of the prevailing bulk price of postconsumer PET to that of virgin bottle-grade PET.[45] Current prices (as of May 2018) for each of these products were obtained from Plastics News[49] and yield an average waste valuation fraction of 0.57 for clear PET and 0.34 for green PET. Owing to the volatility of crude oil prices

and the resulting volatility of plastics prices, the calculated allocation fraction will change over time.

SUPPLEMENTAL INFORMATION

Supplemental Information includes 16 figures, 16 tables, and 1 scheme and can be found with this article online at https://doi.org/10.1016/j.joule.2019.01.018.

ACKNOWLEDGMENTS

This work was authored by Alliance for Sustainable Energy, LLC, the manager and operator of the National Renewable Energy Laboratory for the US Department of Energy (DOE) under contract no. DE-AC36-08GO28308. N.A.R., M.J.B., N.J.G., and G.T.B. thank the NREL Laboratory Directed Research and Development and the US Department of Energy (DOE) Energy Efficiency and Renewable Energy (EERE) Bioenergy Technologies Office (BETO) via contract no. DE-AC36-08GO28308 with the National Renewable Energy Laboratory for funding this work. S.N. and A.C. thank the DOE EERE Advanced Manufacturing Office (AMO) for funding via contract no. DE-AC36-08GO28308 with the National Renewable Energy Laboratory. We thank Davinia Salvachúa for producing the muconic acid used in this work.

AUTHOR CONTRIBUTIONS

N.A.R. synthesized and tested all polymers. N.A.R. and G.T.B. designed the study and wrote the manuscript with input from all co-authors. S.N. and A.C. provided the cradle-to-gate analysis via implementation of the MFI tool. M.J.B. and N.J.G. provided process modeling data on the bioderived monomers.

DECLARATION OF INTERESTS

N.A.R. and G.T.B. have filed a provisional patent on this work and other methods of upcycling PET and possess active patent applications on implementing muconic acid in FRPs (US Provisional Application Nos. 62/327,518 and 62/450,620).

Received: November 2, 2018
Revised: January 10, 2019
Accepted: January 24, 2019
Published: February 27, 2019

REFERENCES

1. Geyer, R., Jambeck, J.R., and Law, K.L. (2017). Production, use, and fate of all plastics ever made. Sci. Adv. *3*, e1700782.

2. Ji, L.N. (2013). Study on preparation process and properties of polyethylene terephthalate (PET). Appl. Mech. Mater. *312*, 406–410.

3. National Association for PET Container Resources, and the Association of Plastic Recyclers. (2015). Report on postconsumer PET container recycling activity in 2014. https://www.plasticsrecycling.org/images/pdf/resources/reports/Rate-Reports/APR_NAPCOR_2014RateReport.pdf.

4. Ormonde, E., Yoneyama, M., and Xu, X. (2016). Plastics recycling. In Chemical Economics Handbook (IHS Market), https://connect.ihs.com/document/show/phoenix/121580.

5. PlasticsEurope. (2016). Plastics - the facts. http://www.plasticseurope.org/Document/plastics—the-facts-2016-15787.aspx?FolID=2.

6. Rillig, M.C. (2012). Microplastic in terrestrial ecosystems and the soil? Environ. Sci. Technol. *46*, 6453–6454.

7. Rochman, C.M. (2018). Microplastics research-from sink to source. Science *360*, 28–29.

8. Eerkes-Medrano, D., Thompson, R.C., and Aldridge, D.C. (2015). Microplastics in freshwater systems: a review of the emerging threats, identification of knowledge gaps and prioritisation of research needs. Water Res. *75*, 63–82.

9. Jambeck, J.R., Geyer, R., Wilcox, C., Siegler, T.R., Perryman, M., Andrady, A., Narayan, R., and Law, K.L. (2015). Marine pollution. Plastic waste inputs from land into the ocean. Science *347*, 768–771.

10. MacArthur, E. (2017). Beyond plastic waste. Science *358*, 843.

11. Ellen MacArthur Foundation. The new plastics economy: rethinking the future of plastics & catalysing action. https://www.ellenmacarthurfoundation.org/publications/the-new-plastics-economy-rethinking-the-future-of-plastics-catalysing-action.

12. Frounchi, M. (1999). Studies on degradation of PET in mechanical recycling. Macromol. Symp. *144*, 465–469.

13. Ávila, A.F., and Duarte, M.V. (2003). A mechanical analysis on recycled PET/HDPE composites. Polym. Degrad. Stab. *80*, 373–382.

14. Koo, H.J., Chang, G.S., Kim, S.H., Hahm, W.G., and Park, S.Y. (2013). Effects of recycling processes on physical, mechanical and

degradation properties of PET yarns. Fibers Polym. *14*, 2083–2087.

15. Welle, F. (2011). Twenty years of PET bottle to bottle recycling—an overview. Resour. Conserv. Recycl. *55*, 865–875.

16. García, J.M. (2016). Catalyst: design challenges for the future of plastics recycling. Chem *1*, 813–815.

17. Garcia, J.M., and Robertson, M.L. (2017). The future of plastics recycling. Science *358*, 870–872.

18. Rahimi, A., and García, J.M. (2017). Chemical recycling of waste plastics for new materials production. Nat. Rev. Chem. *1*, 0046.

19. Karayannidis, G.P., Nikolaidis, A.K., Sideridou, I.D., Bikiaris, D.N., and Achilias, D.S. (2006). Chemical recycling of PET by glycolysis: polymerization and characterization of the dimethacrylated glycolysate. Macromol. Mater. Eng. *291*, 1338–1347.

20. Khoonkari, M., Haghighi, A.H., Sefidbakht, Y., Shekoohi, K., and Ghaderian, A. (2015). Chemical recycling of PET wastes with different catalysts. Int. J. Polym. Sci. *2015*, 1–11, e124524.

21. Sun, J., Liu, D., Young, R.P., Cruz, A.G., Isern, N.G., Schuerg, T., Cort, J.R., Simmons, B.A., and Singh, S. (2017). Solubilization and upgrading of high polyethylene terephthalate loadings in a low-costing bifunctional ionic liquid. ChemSusChem *11*, 781–792.

22. Nyce, G.W., Lamboy, J.A., Connor, E.F., Waymouth, R.M., and Hedrick, J.L. (2002). Expanding the catalytic activity of nucleophilic N-heterocyclic carbenes for transesterification reactions. Org. Lett. *4*, 3587–3590.

23. Hedrick, J.L., Nyce, G.W., and Waymouth, R.M. (2006). Heteroatom-stabilized carbenes and precursors thereto as depolymerization catalysts. US Patent US7053221B2.

24. Kiesewetter, M.K., Shin, E.J., Hedrick, J.L., and Waymouth, R.M. (2010). Organocatalysis: opportunities and challenges for polymer synthesis. Macromolecules *43*, 2093–2107.

25. Fukushima, K., Coulembier, O., Lecuyer, J.M., Almegren, H.A., Alabdulrahman, A.M., Alsewailem, F.D., Mcneil, M.A., Dubois, P., Waymouth, R.M., Horn, H.W., et al. (2011). Organocatalytic depolymerization of poly(ethylene terephthalate). J. Polym. Sci. A Polym. Chem. *49*, 1273–1281.

26. George, N., and Kurian, T. (2014). Recent developments in the chemical recycling of postconsumer poly(ethylene terephthalate) waste. Ind. Eng. Chem. Res. *53*, 14185–14198.

27. Sinha, V., Patel, M.R., and Patel, J.V. (2010). Pet waste management by chemical recycling: a review. J. Polym. Environ. *18*, 8–25.

28. Macijauskas, G., and Jankauskaitė, V. (2013). Epoxy resin and polyurethane compositions from glycolized poly (ethylene terephthalate) wastes. Mater. Sci. *19*, https://doi.org/10.5755/j01.ms.19.3.5237.

29. Attaa, A.M., El-Kafrawy, A.F., Aly, M.H., and Abdel-Azim, A.A. (2007). New epoxy resins based on recycled poly(ethylene terephthalate) as organic coatings. Proc. Org. Coat. *58*, 13–22.

30. Xiao, L., Wang, H., Qian, Q., Jiang, X., Liu, X., Huang, B., and Chen, Q. (2012). Molecular and structural analysis of epoxide-modified recycled poly(ethylene terephthalate) from rheological data. Polym. Eng. Sci. *52*, 2127–2133.

31. Aslan, S., Immirzi, B., Laurienzo, P., Malinconico, M., Martuscelli, E., Volpe, M.G., Pelino, M., and Savini, L. (1997). Unsaturated polyester resins from glycolysed waste polyethyleneterephthalate: synthesis and comparison of properties and performance with virgin resin. J. Mater. Sci. *32*, 2329–2336.

32. Duque-Ingunza, I., López-Fonseca, R., de Rivas, B., and Gutiérrez-Ortiz, J.I. (2013). Synthesis of unsaturated polyester resin from glycolysed postconsumer PET wastes. J. Mater. Cycles Waste Manag. *15*, 256–263.

33. Pimpan, V., Sirisook, R., and Chuayjuljit, S. (2003). Synthesis of unsaturated polyester resin from postconsumer PET bottles: effect of type of glycol on characteristics of unsaturated polyester resin. J. Appl. Polym. Sci. *88*, 788–792.

34. Vaidya, U.R., and Nadkarni, V.M. (1987). Unsaturated polyester resins from poly(ethylene terephthalate) waste. 1. Synthesis and characterization. Ind. Eng. Chem. Res. *26*, 194–198.

35. Vaidya, U.R., and Nadkarni, V.M. (1988). Unsaturated polyester resins from poly(ethylene terephthalate) waste. 2. Mechanical and dynamic mechanical properties. Ind. Eng. Chem. Res. *27*, 2056–2060.

36. Transparency Market Research. Unsaturated polyester resin market - global industry analysis 2013-2019, https://www.transparencymarketresearch.com/unsaturated-polyester-resin.html.

37. Shanks, B.H., and Keeling, P.L. (2017). Bioprivileged molecules: creating value from biomass. Green Chem. *19*, 3177–3185.

38. Rorrer, N.A., Vardon, D.R., Dorgan, J.R., Gjersing, E.J., and Beckham, G.T. (2017). Biomass-derived monomers for performance-differentiated fiber reinforced polymer composites. Green Chem. *19*, 2812–2825.

39. Rorrer, N.A., Dorgan, J.R., Vardon, D.R., Martinez, C.R., Yang, Y., and Beckham, G.T. (2016). Renewable unsaturated polyesters from muconic acid. ACS Sustainable Chem. Eng. *4*, 6867–6876.

40. Mohanty, A.K., Vivekanandhan, S., Pin, J.M., and Misra, M. (2018). Composites from renewable and sustainable resources: challenges and innovations. Science *362*, 536–542.

41. National Renewable Energy Laboratory. (2012). US life cycle inventory database. https://www.nrel.gov/lci/.

42. Hanes, R.J., and Carpenter, A. (2017). Evaluating opportunities to improve material and energy impacts in commodity supply chains. Environ. Syst. Decis. *37*, 6–12.

43. US Energy Information Administration. (2018). Annual energy outlook. https://www.eia.gov/outlooks/aeo/pdf/AEO2018.pdf.

44. Piccinno, F., Hischier, R., Seeger, S., and Som, C. (2016). From laboratory to industrial scale: a scale-up framework for chemical processes in life cycle assessment studies. J. Clean. Prod. *135*, 1085–1097.

45. Shen, L., Worrell, E., and Patel, M.K. (2010). Open-loop recycling: a LCA case study of PET bottle-to-fibre recycling. Resour. Conserv. Recycl. *55*, 34–52.

46. Karp, E.M., Eaton, T.R., Nogue, V.S.i., Vorotnikov, V., Biddy, M.J., Tan, E.C.D., Brandner, D.G., Cywar, R.M., Liu, R., Manker, L.P., et al. (2017). Renewable acrylonitrile production. Science *358*, 1307–1310.

47. Yim, H., Haselbeck, R., Niu, W., Pujol-Baxley, C., Burgard, A., Boldt, J., Khandurina, J., Trawick, J.D., Osterhout, R.E., Stephen, R., et al. (2011). Metabolic engineering of Escherichia coli for direct production of 1,4-butanediol. Nat. Chem. Biol. *7*, 445–452.

48. HIS Markit. Chemical process economics program PEP. https://ihsmarkit.com/products/chemical-technology-pep-index.html.

49. Plastics News. Commodity thermoplastics - resin pricing. http://www.plasticsnews.com/resin/commodity-thermoplastics/current-pricing.

50. Plastics News. Thermosets - resin pricing. http://www.plasticsnews.com/resin/thermosets/current-pricing.

51. Reportlinker unsaturated polyester resin - Asia pacific industry analysis, size, share, growth, trends and forecast 2015-2023. http://www.prnewswire.com/news-releases/unsaturated-polyester-resin—asia-pacific-industry-analysis-size-share-growth-trends-and-forecast-2015—2023-300211023.html.

52. Karbhari, V.M., and Zhao, L. (2000). Use of composites for 21st century civil infrastructure. Comput. Methods Appl. Mech. Eng. *185*, 433–454.

53. National Toxicology Program. (2011). NTP 12th report on carcinogens. Rep. Carcinog. *12*, iii–499.

54. Claypool, J.T., Raman, D.R., Jarboe, L.R., and Nielsen, D.R. (2014). Technoeconomic evaluation of bio-based styrene production by engineered Escherichia coli. J. Ind. Microbiol. Biotechnol. *41*, 1211–1216.

55. Lian, J., McKenna, R., Rover, M.R., Nielsen, D.R., Wen, Z., and Jarboe, L.R. (2016). Production of biorenewable styrene: utilization of biomass-derived sugars and insights into toxicity. J. Ind. Microbiol. Biotechnol. *43*, 595–604.

56. Liu, C., Men, X., Chen, H., Li, M., Ding, Z., Chen, G., Wang, F., Liu, H., Wang, Q., Zhu, Y., et al. (2018). A systematic optimization of styrene biosynthesis in Escherichia coli BL21. Biotechnol. Biofuels *11*, 14.

57. Carlsson, M., Habenicht, C., Kam, L.C., Antal, M.J.J., Bian, N., Cunningham, R.J., and Jones, M.J. (1994). Study of the sequential conversion of citric to itaconic to methacrylic acid in near-critical and supercritical water. Ind. Eng. Chem. Res. *33*, 1989–1996.

58. Lansing, J.C., Murray, R.E., and Moser, B.R. (2017). Biobased methacrylic acid via selective catalytic decarboxylation of itaconic acid. ACS Sustainable Chem. Eng. *5*, 3132–3140.

59. Li, P., Ma, S., Dai, J., Liu, X., Jiang, Y., Wang, S., Wei, J., Chen, J., and Zhu, J. (2017). Itaconic acid as a green alternative to acrylic acid for producing a soybean oil-based thermoset: synthesis and properties. ACS Sustainable Chem. Eng. *5*, 1228–1236.

60. Willke, T., and Vorlop, K.D. (2001). Biotechnological production of itaconic acid. Appl. Microbiol. Biotechnol. *56*, 289–295.

61. Steiger, M.G., Blumhoff, M.L., Mattanovich, D., and Sauer, M. (2013). Biochemistry of microbial itaconic acid production. Front. Microbiol. *4*, 23.

62. Beerthuis, R., Rothenberg, G., and Shiju, N.R. (2015). Catalytic routes towards acrylic acid, adipic acid and ε-caprolactam starting from biorenewables. Green Chem. *17*, 1341–1361.

63. Mok, W.S.L., Antal, M.J., and Jones, M. (1989). Formation of acrylic acid from lactic acid in supercritical water. J. Org. Chem. *54*, 4596–4602.

64. Zhang, J., Lin, J., and Cen, P. (2008). Catalytic dehydration of lactic acid to acrylic acid over sulfate catalysts. Can. J. Chem. Eng. *86*, 1047–1053.

65. European Chemicals Bureau, Institute for Health and Consumer Protection. (2002). European union risk assessment report - methacrylic acid. https://echa.europa.eu/documents/10162/f0b94b4b-a87b-442b-b647-8ff56895c92c.

66. Cousinet, S., Ghadban, A., Fleury, E., Lortie, F., Pascault, J.-P., and Portinha, D. (2015). Toward replacement of styrene by bio-based methacrylates in unsaturated polyester resins. Eur. Polym. J. *67*, 539–550.

67. He, S.L., Yaszemski, M.J., Yasko, A.W., Engel, P.S., and Mikos, A.G. (2000). Injectable biodegradable polymer composites based on poly(propylene fumarate) crosslinked with poly(ethylene glycol)-dimethacrylate. Biomaterials *21*, 2389–2394.

68. Bevington, J.C., Colley, F.R., and Ebdon, J.R. (1973). Copolymers of methyl methacrylate with cinnamic acid. Polymer *14*, 409–410.

69. Schutyser, W., Renders, T., Van den Bosch, S., Koelewijn, S.F., Beckham, G.T., and Sels, B.F. (2018). Chemicals from lignin: an interplay of lignocellulose fractionation, depolymerisation, and upgrading. Chem. Soc. Rev. *47*, 852–908.

70. Parsell, T., Yohe, S., Degenstein, J., Jarrell, T., Klein, I., Gencer, E., Hewetson, B., Hurt, M., Kim, J.I., Choudhari, H., et al. (2015). A synergistic biorefinery based on catalytic conversion of lignin prior to cellulose starting from lignocellulosic biomass. Green Chem. *17*, 1492–1499.

71. Anderson, E.M., Katahira, R., Reed, M., Resch, M.G., Karp, E.M., Beckham, G.T., and Román-Leshkov, Y. (2016). Reductive catalytic fractionation of corn Stover lignin. ACS Sustainable Chem. Eng. *4*, 6940–6950.

72. Beckham, G.T., Johnson, C.W., Karp, E.M., Salvachúa, D., and Vardon, D.R. (2016). Opportunities and challenges in biological lignin valorization. Curr. Opin. Biotechnol. *42*, 40–53.

73. Song, Q., Wang, F., Cai, J., Wang, Y., Zhang, J., Yu, W., and Xu, J. (2013). Lignin depolymerization (LDP) in alcohol over nickel-based catalysts via a fragmentation–hydrogenolysis process. Energy Environ. Sci. *6*, 994.

74. Ahvazi, B., Cloutier, É., Wojciechowicz, O., and Ngo, T.-D. (2016). Lignin profiling: a guide for selecting appropriate lignins as precursors in biomaterials development. ACS Sustainable Chem. Eng. *4*, 5090–5105.

75. Ragauskas, A.J., Beckham, G.T., Biddy, M.J., Chandra, R., Chen, F., Davis, M.F., Davison, B.H., Dixon, R.A., Gilna, P., Keller, M., et al. (2014). Lignin valorization: improving lignin processing in the biorefinery. Science *344*, 1246843.

76. Zakzeski, J., Bruijnincx, P.C.A., Jongerius, A.L., and Weckhuysen, B.M. (2010). The catalytic valorization of lignin for the production of renewable chemicals. Chem. Rev. *110*, 3552–3599.

77. Van den Bosch, S., Schutyser, W., Vanholme, R., Driessen, T., Koelewijn, S.-F., Renders, T., De Meester, B., Huijgen, W.J.J., Dehaen, W., Courtin, C.M., et al. (2015). Reductive lignocellulose fractionation into soluble lignin-derived phenolic monomers and dimers and processable carbohydrate pulps. Energy Environ. Sci. *8*, 1748–1763.

78. George, A., Brandt, A., Tran, K., Zahari, S.M.S.N.S., Klein-Marcuschamer, D., Sun, N., Sathitsuksanoh, N., Shi, J., Stavila, V., Parthasarathi, R., et al. (2015). Design of low-cost ionic liquids for lignocellulosic biomass pretreatment. Green Chem. *17*, 1728–1734.

79. Ma, R., Xu, Y., and Zhang, X. (2015). Catalytic oxidation of biorefinery lignin to value-added chemicals to support sustainable biofuel production. ChemSusChem *8*, 24–51.

80. Huang, Y.-J., and Jiang, W.-C. (1998). Effects of chemical composition and structure of unsaturated polyester resins on the miscibility, cured sample morphology and mechanical properties for styrene/unsaturated polyester/low-profile additive ternary systems. 1: Miscibility and cured sample morphology. Polymer *39*, 6631–6641.

81. Malik, M., Choudhary, V., and Varma, I.K. (2000). Current status of unsaturated polyester resins. J. Macromol. Sci. Polym. Rev. *40*, 139–165.

82. Xi, J., Ding, D., Shao, Y., Liu, X., Lu, G., and Wang, Y. (2014). Production of ethylene glycol and its monoether derivative from cellulose. ACS Sustain. Chem. Eng. *2*, 2355–2362.

83. Mückschel, B., Simon, O., Klebensberger, J., Graf, N., Rosche, B., Altenbuchner, J., Pfannstiel, J., Huber, A., and Hauer, B. (2012). Ethylene glycol metabolism by Pseudomonas putida. Appl. Environ. Microbiol. *78*, 8531–8539.

84. Pereira, B., Li, Z.J., De Mey, M., Lim, C.G., Zhang, H., Hoeltgen, C., and Stephanopoulos, G. (2016). Efficient utilization of pentoses for bioproduction of the renewable two-carbon compounds ethylene glycol and glycolate. Metab. Eng. *34*, 80–87.

85. Cabulong, R.B., Valdehuesa, K.N.G., Ramos, K.R.M., Nisola, G.M., Lee, W.K., Lee, C.R., and Chung, W.J. (2017). Enhanced yield of ethylene glycol production from D-xylose by pathway optimization in Escherichia coli. Enzyme Microb. Technol. *97*, 11–20.

86. Van Uytvanck, P.P., Haire, G., Marshall, P.J., and Dennis, J.S. (2017). Impact on the polyester value chain of using p-xylene derived from biomass. ACS Sustainable Chem. Eng. *5*, 4119–4126.

87. Frost, J.W., Miermont, A., Schweitzer, D., and Bui, V. (2013). Preparation of trans, trans muconic acid and trans, trans muconates. US patent: US8426639B2.

88. Matthiesen, J.E., Carraher, J.M., Vasiliu, M., Dixon, D.A., and Tessonnier, J.-P. (2016). Electrochemical conversion of muconic acid to biobased diacid monomers. ACS Sustainable Chem. Eng. *4*, 3575–3585.

89. Carraher, J.M., Pfennig, T., Rao, R.G., Shanks, B.H., and Tessonnier, J. (2017). cis,cis -muconic acid isomerization and catalytic conversion to biobased cyclic-C 6 -1,4-diacid monomers. Green Chem. *19*, 3042–3050.

90. Settle, A.E., Berstis, L., Rorrer, N.A., Roman-Leshkóv, Y., Beckham, G.T., Richards, R.M., and Vardon, D.R. (2017). Heterogeneous Diels–Alder catalysis for biomass-derived aromatic compounds. Green Chem. *19*, 3468–3492.

91. Settle, A.E., Berstis, L., Zhang, S., Rorrer, N.A., Hu, H., Richards, R.M., Beckham, G.T., Crowley, M.F., and Vardon, D.R. (2018). Iodine-catalyzed isomerization of dimethyl muconate. ChemSusChem *11*, 1768–1780.

92. Bechthold, I., Bretz, K., Kabasci, S., Kopitzky, R., and Springer, A. (2008). Succinic acid: a new platform chemical for biobased polymers from renewable resources. Chem. Eng. Technol. *31*, 647–654.

93. Kang, K.H., Hong, U.G., Bang, Y., Choi, J.H., Kim, J.K., Lee, J.K., Han, S.J., and Song, I.K. (2015). Hydrogenation of succinic acid to 1,4-butanediol over Re–Ru bimetallic catalysts supported on mesoporous carbon. Applied Catalysis A: General *490*, 153–162.

94. Vardon, D.R., Settle, A.E., Vorotnikov, V., Menart, M.J., Eaton, T.R., Unocic, K.A., Steirer, K.X., Wood, K.N., Cleveland, N.S., Moyer, K.E., et al. (2017). Ru-Sn/AC for the aqueous-phase reduction of succinic acid to 1,4-butanediol under continuous process conditions. ACS Catal. *7*, 6207–6219.

95. Liu, D.(J.), and Chen, E.Y.-X. (2014). Integrated catalytic process for biomass conversion and upgrading to C 12 furoin and alkane fuel. ACS Catal. *4*, 1302–1310.

96. He, J., Huang, K., Barnett, K.J., Krishna, S.H., Alonso, D.M., Brentzel, Z.J., Burt, S.P., Walker, T., Banholzer, W.F., Maravelias, C.T., et al. (2017). New catalytic strategies for α,ω-diols production from lignocellulosic biomass. Faraday Discuss. *202*, 247–267.

97. Rose, M., and Palkovits, R. (2012). Isosorbide as a renewable platform chemical for versatile applications—quo vadis? ChemSusChem *5*, 167–176.

98. Carta, F.S., Soccol, C.R., Ramos, L.P., and Fontana, J.D. (1999). Production of fumaric acid by fermentation of enzymatic hydrolysates derived from cassava bagasse. Bioresour. Technol. *68*, 23–28.

99. Roa Engel, C.A., Straathof, A.J.J., Zijlmans, T.W., van Gulik, W.M., and van der Wielen, L.A.M. (2008). Fumaric acid production by fermentation. Appl. Microbiol. Biotechnol. *78*, 379–389.

100. Xu, Q., Li, S., Huang, H., and Wen, J. (2012). Key technologies for the industrial production of fumaric acid by fermentation. Biotechnol. Adv. *30*, 1685–1696.

101. Saraçi, E., Wang, L., Theopold, K.H., and Lobo, R.F. (2018). Bioderived muconates by cross-metathesis and their conversion into terephthalates. ChemSusChem *11*, 773–780.

102. Zhu, T., Li, Z., Xiao, F., and Duan, W.-L. (2018). Pd-catalyzed oxidative homo-coupling of acrylates and aromatic alkenes for the conjugated diene synthesis. Tetrahedron Lett. *59*, 3238–3241.

103. Lu, R., Lu, F., Chen, J., Yu, W., Huang, Q., Zhang, J., and Xu, J. (2016). Production of diethyl terephthalate from biomass-derived muconic acid. Angew. Chem. Int. Ed. *55*, 249–253.

104. Feuer, S.S., Bockstahler, T.E., Brown, C.A., and Rosenthal, I. (1954). Maleic-fumaric isomerization in unsaturated polyesters. Ind. Eng. Chem. *46*, 1643–1645.

105. Dai, J., Ma, S., Teng, N., Dai, X., Shen, X., Wang, S., Liu, X., and Zhu, J. (2017). 2,5-Furandicarboxylic acid- and itaconic acid-derived fully biobased unsaturated polyesters and their cross-linked networks. Ind. Eng. Chem. Res. *56*, 2650–2657.

106. Madival, S., Auras, R., Singh, S.P., and Narayan, R. (2009). Assessment of the environmental profile of PLA, PET and PS clamshell containers using LCA methodology. J. Clean. Prod. *17*, 1183–1194.

107. Tabone, M.D., Cregg, J.J., Beckman, E.J., and Landis, A.E. (2010). Sustainability metrics: life cycle assessment and green design in polymers. Environ. Sci. Technol. *44*, 8264–8269.

108. Laurent, A., Bakas, I., Clavreul, J., Bernstad, A., Niero, M., Gentil, E., Hauschild, M.Z., and Christensen, T.H. (2014). Review of LCA studies of solid waste management systems – part I: lessons learned and perspectives. Waste Manag. *34*, 573–588.

109. Laurent, A., Clavreul, J., Bernstad, A., Bakas, I., Niero, M., Gentil, E., Christensen, T.H., and Hauschild, M.Z. (2014). Review of LCA studies of solid waste management systems – part II: methodological guidance for a better practice. Waste Manag. *34*, 589–606.

110. Joint Research Centre, European Commission. (2017). Energy efficiency and GHG emissions: prospective scenarios for the chemical and petrochemical industry. https://publications.europa.eu/en/publication-detail/-/publication/dabfc65f-31cc-11e7-9412-01aa75ed71a1/language-en.

111. IHS Markit. Polyester resins, unsaturated - chemical economics handbook (CEH). https://ihsmarkit.com/products/unsaturated-polyester-resins-chemical-economics-handbook.html.

112. Ji, N., Zhang, T., Zheng, M., Wang, A., Wang, H., Wang, X., and Chen, J.G. (2008). Direct catalytic conversion of cellulose into ethylene glycol using nickel-promoted tungsten carbide catalysts. Angew. Chem. Int. Ed. *47*, 8510–8513.

113. Zheng, M., Pang, J., Sun, R., Wang, A., and Zhang, T. (2017). Selectivity control for cellulose to diols: dancing on eggs. ACS Catal. *7*, 1939–1954.

114. Vardon, D.R., Franden, M.A., Johnson, C.W., Karp, E.M., Guarnieri, M.T., Linger, J.G., Salm, M.J., Strathmann, T.J., and Beckham, G.T. (2015). Adipic acid production from lignin. Energy Environ. Sci. *8*, 617–628.

115. Corona, A., Biddy, M.J., Vardon, D.R., Birkved, M., Hauschild, M.Z., and Beckham, G.T. (2018). Life cycle assessment of adipic acid production from lignin. Green Chem. *20*, 3857–3866.